Growth of Ruddlesden-Popper phase $La_4Ni_3O_{10}$ thin film on $LaAlO_3$ substrate via pulsed laser deposition method

*Ryo Matsumoto[1], Souma Kodani[3+], Eiji Hitsuda[1,4], Yuki Nishimiya[2], Yoshihiro Nemoto[2], Yoshihiko Takano[1,4], Hiromi Tanaka[3]

*Corresponding author; Email: MATSUMOTO.Ryo@nims.go.jp

[1]International Center for Materials Nanoarchitectonics (MANA), National Institute for Materials Science, Tsukuba, Ibaraki 305-0047, Japan

[2]Research Network and Facility Services Division, National Institute for Materials Science, Tsukuba, Ibaraki 305-0047, Japan

[3]National Institute of Technology, Yonago College, Yonago, Tottori 683-8502, Japan

[4]Graduate School of Science and Technology, University of Tsukuba, 1-1-1 Tennodai, Tsukuba, Ibaraki 305-8577, Japan

+Present address; Graduate School of Engineering, Tohoku University, Sendai, 980-0845, Japan

Abstract

Pulsed laser deposition (PLD) is a promising technique for thin-film growth from the perspectives of both practical applications and the development of fundamental materials science. Recently, $La_3Ni_2O_7$ thin films, belonging to the layered Ruddlesden–Popper (RP) nickelates $La_{n+1}Ni_nO_{3n+1}$, grown on substrates inducing compressive strain due to lattice mismatch, have attracted considerable attention as a new class of high transition-temperature superconductors at ambient pressure. Although the emergence of superconductivity in the related RP-type nickelate $La_4Ni_3O_{10}$ thin film is anticipated, the growth of an oriented thin film along the c-axis with compressive strain has not been reported by using the PLD process. In this study, we investigate the thin-film growth of $La_4Ni_3O_{10}$ using the PLD technique on a $LaAlO_3$ substrate, which imposes a compressive strain. X-ray diffraction analysis and transmission electron microscopy reveal that well-oriented $La_4Ni_3O_{10}$ phases can be grown on the $LaAlO_3$ substrate. Although superconductivity is absent in the grown film, the phase formation of $La_4Ni_3O_{10}$ on the $LaAlO_3$ substrate via the PLD process is the first step for the realization of ambient-pressure superconductivity in this system.

1. Introduction

The development of functional materials plays a central role in advancing modern technology and improving the quality of life. Among various material forms, thin films are particularly important for device applications because of their compatibility with integration and large-scale production. Epitaxial thin films on single-crystalline substrates are typically grown by techniques such as chemical vapor deposition (CVD), metal–organic decomposition (MOD), and molecular beam epitaxy (MBE), depending on the target material[1,2]. Pulsed laser deposition (PLD) is another widely used method for fabricating functional thin films, including semiconductors[3], solid ionic conductors[4], optoelectronic materials[5], and superconducting devices[6]. PLD offers several advantages, such as a relatively simple process using a bulk target, high compositional homogeneity over large substrates, and flexibility of the deposition environment[7,8]. In addition, epitaxial growth under lattice mismatch enables access to metastable phases stabilized by substrate-induced strain, providing a powerful route to discovering novel functional materials[9]. For these reasons, PLD has become a promising tool not only for device applications but also for fundamental studies in condensed matter physics.

Layered Ruddlesden–Popper (RP) nickelates, $RE_{n+1}Ni_nO_{3n+1}$ (*RE* = rare-earth element), have long been investigated as functional materials, particularly for applications in solid oxide fuel cells[10]. Recently, the $n = 2$ member, $La_3Ni_2O_7$, has attracted considerable attention following the discovery of superconductivity with a transition temperature (T_c) exceeding 80 K under high pressure[11], above the boiling point of liquid nitrogen. The orthorhombic structure of non-superconducting $La_3Ni_2O_7$ undergoes to a superconducting tetragonal structure through a structural modification above 8 GPa[12]. Many experimental and theoretical research have been conducted to investigate the superconducting mechanism and possible enhancement of T_c[13–21]. In parallel, efforts have been directed toward realizing superconductivity in $La_3Ni_2O_7$ at ambient pressure for practical applications. Most recently, superconducting $La_3Ni_2O_7$ thin films with T_c above 40 K at ambient pressure were achieved by epitaxial growth on $SrLaAlO_4$ substrates using PLD[22–24]. In this case, lattice mismatch–induced strain plays a role analogous to external pressure, stabilizing the superconducting phase. The realization of superconductivity at ambient pressure in the RP nickelate thin film has opened new opportunities for quantum device research using the PLD method.

Following the discovery of high-T_c superconductivity in compressed $La_3Ni_2O_7$, pressure-induced superconductivity with T_c above 30 K has also been reported in the $n = 3$ RP nickelate $La_4Ni_3O_{10}$, again associated with a pressure-driven structural modification at around 20 GPa[25–28]. By analogy with $La_3Ni_2O_7$, the development of superconducting $La_4Ni_3O_{10}$ thin films using PLD is highly anticipated. However, the epitaxial growth of $La_4Ni_3O_{10}$ thin films on a specific substrate with a smaller in-plane lattice constant than that of $La_4Ni_3O_{10}$ by PLD has not yet been systematically investigated. In this work, we examine the growth conditions for $La_4Ni_3O_{10}$ thin films with 00*l* orientation on $LaAlO_3$ (LAO) substrates, which induces a large lattice mismatch, using the PLD

method. X-ray diffraction (XRD) analysis reveals that the oriented film of $La_4Ni_3O_{10}$ along the c-axis is mainly grown on the LAO substrate. Local structural analysis indicates that the dominant region of the film is the $La_4Ni_3O_{10}$ phase, with minor contributions from the other phases and local defects. films. By changing the parameters of the PLD process, a different layer number of $La_3Ni_2O_7$ (n = 2) was grown as a byproduct. Electrical transport measurements demonstrate a reduction of the band gap with increasing layer number n. These findings provide important insights into the growth and electronic structure of RP nickelate thin films and represent a key step toward the realization of superconducting $La_4Ni_3O_{10}$ thin films by PLD.

2. Expetimental procedures

$La_4Ni_3O_{10}$ (n = 3) thin films were grown on 00l-oriented $LaAlO_3$ substrates by the PLD using a polycrystalline $La_4Ni_3O_{10}$ target. The target was prepared by repeated solid-state reactions of La_2O_3 and NiO powders mixed in a molar ratio of 2:3. The mixed powders were calcined and sintered in air at 1200°C for 24 h. Thin-film growth was carried out using a PLD system (PAC-LMBE, PASCAL Co.) equipped with a Nd:YAG laser (λ = 1064 nm). During deposition, the laser repetition rate, substrate temperature (T_{sub}), oxygen partial pressure (P_{O2}), laser power, and distance between the target and substrate (D_{ts}) were varied to optimize growth conditions. The growth conditions in this paper are summarized in Table S1.

The crystal structure of the obtained films was characterized by X-ray diffraction (XRD) using a SmartLab diffractometer (Rigaku) with monochromated Cu $K_{\alpha1}$ radiation (λ = 1.5406 Å). The temperature dependence of the electrical resistance was measured by a standard four-probe method with a collinear geometry using Au wires attached with Ag paste in a physical property measurement system (Quantum Design). Transmission electron microscopy (TEM) and atomic-resolution energy-dispersive X-ray spectroscopy (EDX) mapping were performed using a JEM-ARM200F microscope (JEOL). Cross-sectional TEM specimens were prepared by focused ion beam (FIB) milling using a JIB-4000 system (JEOL).

3. Results and discussion

Figure 1 shows an XRD pattern obtained by a θ–2θ scan of the $La_4Ni_3O_{10}$ thin film on the LAO substrate deposited under the conditions of T_{sub} = 690°C and P_{O2} = 20 Pa. The laser power and D_{ts} were set to 33 mJ and 30 mm, respectively. The film thickness of 93 nm was obtained with 6000 laser pulses, estimated via TEM analysis as discussed later. The film clearly exhibits (00l) diffraction peaks originating from the RP-type structure of $La_4Ni_3O_{10}$, indicating that the film is highly oriented along the c-axis. A peak position at around 47° with a square symbol among the tiny unknown peaks is near that from (002) diffraction of $LaNiO_3$. Other tiny and sharp unknown peaks possibly originate from an extrinsic component, for example, Ag paste for the bond of the substrate to the sample holder of

PLD. The crystal structure of the LAO substrate is rhombohedral, and can be approximated as a pseudo-cubic structure with a_{LAO} = 3.787 Å[29]. On the other hand, bulk $La_4Ni_3O_{10}$ has an orthorhombic *Amam* structure with lattice parameters a = 5.415 Å, b = 5.465 Å, and c = 27.96 Å[30]. This structure can be approximated by a pseudo-tetragonal unit cell with $a_{4310} = b_{4310}$ = 3.847 Å and c_{4310} = 27.96 Å. From this lattice mismatch, a compressive strain of −1.6% is expected to be applied to the $La_4Ni_3O_{10}$ thin film grown on the LAO substrate. In the case of $La_3Ni_2O_7$ films, the critical compressive strain for the emergence of superconductivity at ambient pressure has been reported to be between −1.2% and −2.1%[23]. The strain of −1.6% in the $La_4Ni_3O_{10}$ film on the LAO substrate lies within this critical range reported for $La_3Ni_2O_7$ films, suggesting that epitaxial strain may significantly influence the electronic states. Consistently, the out-of-plane lattice constant of the obtained film is estimated to be c = 28.45 Å, which indicates the elongation of 1.8% compared with the bulk value due to the in-plane compressive strain. Such an elongation of the *c*-axis is commonly observed in epitaxial thin films under compressive strain and has also been reported in superconducting $La_3Ni_2O_7$ films[31]. These results indicate that the epitaxial strain imposed by the LAO substrate effectively modifies the lattice structure of $La_4Ni_3O_{10}$, which may provide a platform for tuning its electronic properties.

RP-type nickelates exhibit a complex phase diagram including n = 1, 2, 3, and ∞ within a narrow growth window. During the modification of the growth conditions in the PLD process, the $La_3Ni_2O_7$ thin film is also obtained as the byproduct even with the same target composition as shown in the bottom XRD pattern in Fig. 1. The film thickness is estimated to be approximately 50 nm, since the number of laser pulses used for deposition was half that of the $La_4Ni_3O_{10}$ film. The main difference is a change in the value of PLD parameters, such as the D_{ts} from 30 mm to 40 mm, the P_{O2} from 20 Pa to 35 Pa, and the T_{sub} from 690°C to 720°C. The n value of RP-type nickelates tends to decrease with increasing T_{sub} and decreasing P_{O2} in the phase diagram[32]. Although the $La_4Ni_3O_{10}$ phase seems to be more stable under these conditions because the higher P_{O2} contributes to increase n value and the difference in T_{sub} is slight, the $La_3Ni_2O_7$ phase obviously appears. This result suggests that the increase in D_{ts} is considered to be the primary factor promoting the formation of the $La_3Ni_2O_7$ phase. Previous studies have reported that lighter elements tend to be scattered farther away from the target-to-substrate direction than heavier elements[33]. As a result, the concentration of lighter elements in deposited films is reduced. Because this effect may become more pronounced with increasing D_{ts}, the formation of the Ni-deficient phase $La_3Ni_2O_7$ is likely facilitated when D_{ts} is increased from 30 mm to 40 mm.

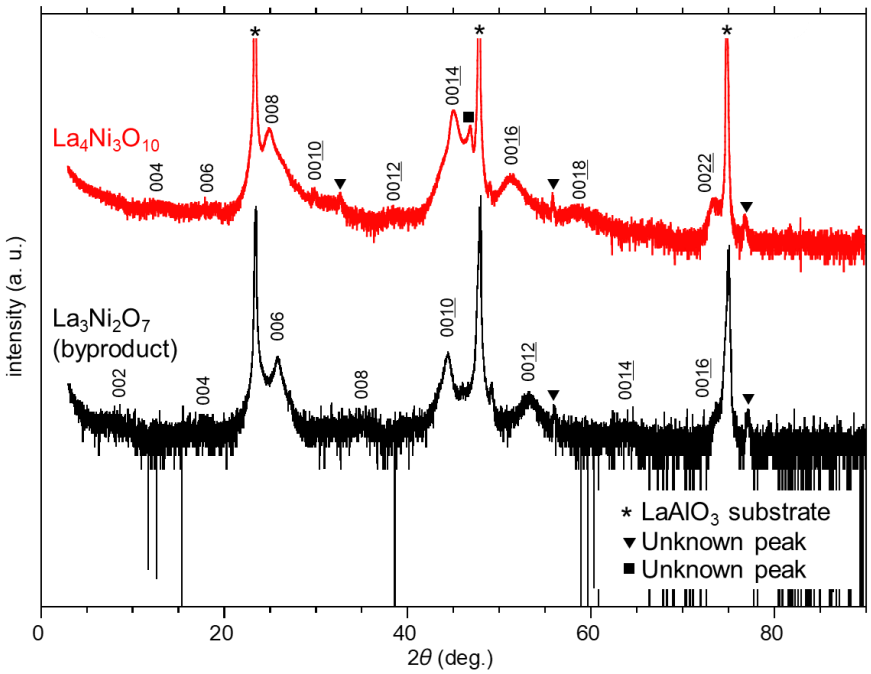


FIG. 1. XRD pattern using a θ–2θ scan of the $La_4Ni_3O_{10}$ and $La_3Ni_2O_7$ thin film on the LAO substrate. The asterisks indicate diffraction peaks from the LAO substrate.

The local structure of the obtained $La_4Ni_3O_{10}$ thin film was analyzed by TEM observation. A tiny square region was picked up from the surface of the substrate and fabricated into an extremely thin specimen using the FIB process to perform high-resolution TEM analysis, as shown in the scanning ion microscope images in Fig. 2(a) and (b). The cross-section of the sample was analyzed using a high-angle annular dark-field scanning TEM image, as shown in Fig. 2(c). The top region corresponds to the surface of the film, and the bottom region corresponds to the boundary between the grown film and the LAO substrate. The film thickness is 93 nm. Among the analyzed regions, the crystal growth of $La_4Ni_3O_{10}$ is observed as the main phase, which is consistent with the XRD measurements. In addition, small regions of La_2NiO_4, $La_3Ni_2O_7$, and amorphous-like distorted structures are observed. For instance, the $La_3Ni_2O_7$ phase is partially observed at around the boundary between the deposited film and the LAO substrate, as shown in Fig. S1. The appearance of other RP-type nickelate phases strongly depends on the parameters of the PLD process, as discussed later. The use of a lower laser repetition frequency may also enhance the quality of the grown crystal, although it was limited in the present experiments due to problems with the PLD equipment. Figure 2(d) shows an enlarged TEM image around the $La_4Ni_3O_{10}$ region. The brightest atomic columns correspond to lanthanum atoms, while the darker ones correspond to nickel atoms, which are identified by atomic-resolution EDX mapping, as shown in Fig. 2(e). In the EDX mapping, red and green indicate lanthanum and nickel, respectively. Based on these TEM observations, the $La_4Ni_3O_{10}$ thin film with (00l) orientation is clearly grown on the LAO substrate using the PLD process.

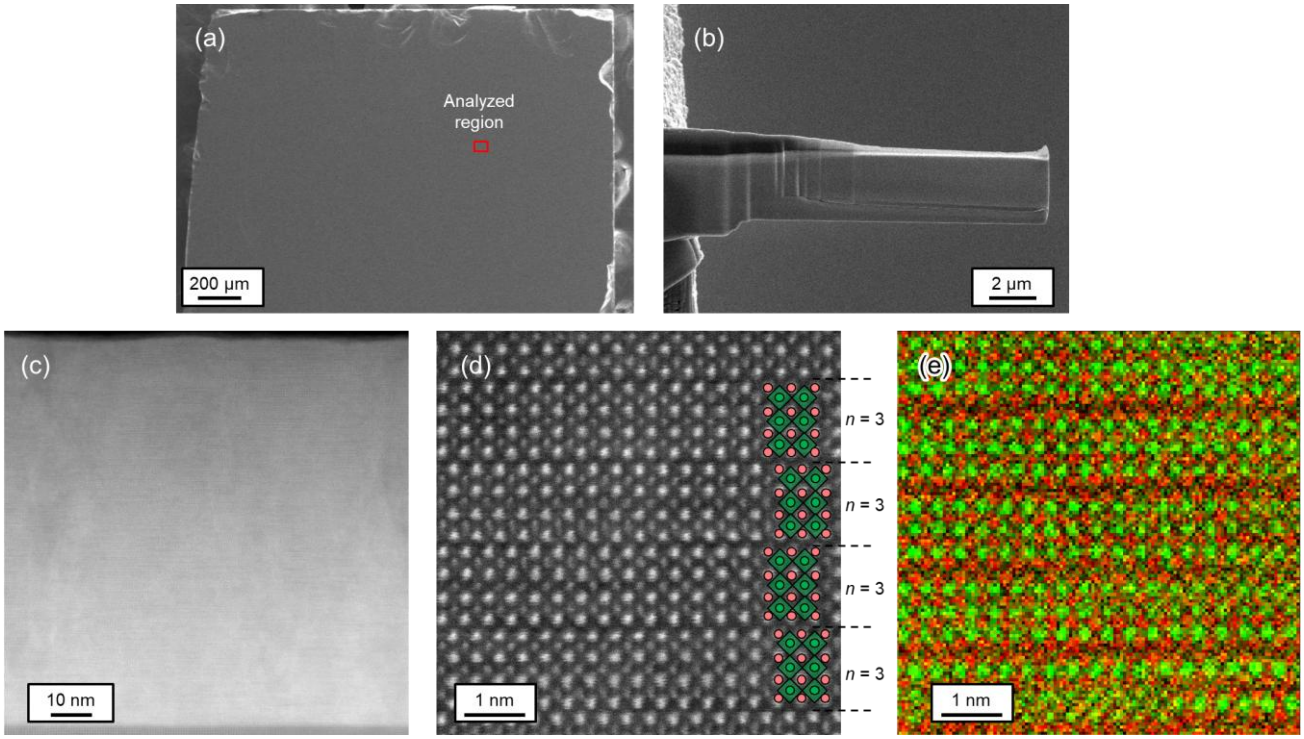


FIG. 2. Scanning ion microscope images of the (a) analyzed region and (b) fabricated specimen of $La_4Ni_3O_{10}$ thin film on the LAO substrate for TEM observation. (c) High-angle annular dark-field scanning TEM images for the entire region from the substrate to the surface and (d) a specific region containing $La_4Ni_3O_{10}$. (e) Atomic-resolution EDX mapping image of the $La_4Ni_3O_{10}$ region. Red and Green colors indicate lanthanum and nickel atoms, respectively.

Figure 3(a) shows the temperature dependence of the electrical resistance for the $La_3Ni_2O_7$ and $La_4Ni_3O_{10}$ films. Both films exhibit an increasing trend in resistance with decreasing temperature, namely semiconducting-like behavior without a superconducting transition. Because the thickness of the deposited films was not accurately determined due to the existence of a minor phase as indicated in the TEM observation, the electrical resistance is shown instead of resistivity. Although a direct comparison of electrical resistivity is difficult, the measured resistance was analyzed using the Arrhenius relationship, $R=R_0\times\exp(E_a/k_BT)$, where R_0 is the residual resistivity, E_a is the activation energy, k_B is the Boltzmann constant and T is the temperature, as shown in the Fig. 3 (b). The linear fit around room temperature yields activation energies E_a of 38 meV and 18 meV for $La_3Ni_2O_7$ and $La_4Ni_3O_{10}$, respectively. These results indicate that the E_a tends to decrease with increasing n in RP-type nickelates. In the case of $La_3Ni_2O_7$ thin films, the bandgap drastically decreases by tuning the carrier concentration through the O_3 annealing process, and metallic superconducting phases appear under very narrow optimal conditions[22–24]. Following the $La_3Ni_2O_7$ case, carrier tuning by O_3 annealing may also be effective for inducing superconductivity in $La_4Ni_3O_{10}$ thin films. Although the O_3 annealing around 300°C inside the PLD chamber contributes to the reduction of the resistance, as shown in Fig. 3(c), no superconducting transition is observed in the $La_4Ni_3O_{10}$ thin film. The reduction

in resistance induced by O_3 annealing gradually recovers over a period of two months, as shown in Fig. S2. This aging effect is consistent with previous reports on superconducting $La_3Ni_2O_7$ thin films and suggests that the resistance reduction originates from carrier doping rather than the presence of metallic impurity phases such as $LaNiO_3$. As a future investigation, exploring the optimal conditions of O_3 annealing to tune the carrier concentration in $La_4Ni_3O_{10}$ thin films may open the possibility of achieving superconductivity without external pressure.

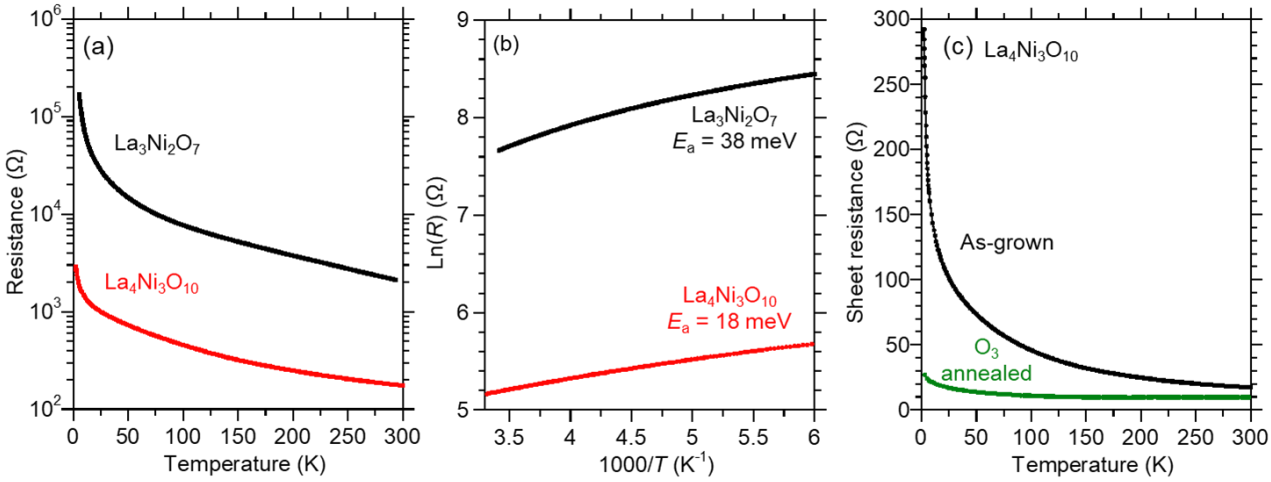


FIG. 3. (a) Temperature dependence of electrical resistance for the obtained films with the main phase $La_3Ni_2O_7$ and $La_4Ni_3O_{10}$. (b) The Arrhenius relationship at around room temperature. (c) Temperature dependence of the sheet resistance of the as-grown $La_4Ni_3O_{10}$ film and the O_3-annealed one.

4. Conclusion

The thin-film growth of RP-type $La_4Ni_3O_{10}$ on an LAO substrate is investigated using the PLD method. XRD analysis reveals that an oriented $La_4Ni_3O_{10}$ film along the c-axis is grown on the LAO substrate as the main phase. The elongation of the c-axis provides possible evidence of compressive strain induced between the deposited film and the substrate. The local structure of the film is analyzed by TEM, where the crystal growth of $La_4Ni_3O_{10}$ is confirmed by atomic-resolution column imaging and EDX mapping. Minor phases of other RP-type nickelates, La_2NiO_4 and $La_3Ni_2O_7$, are also observed. By using different PLD conditions, $La_3Ni_2O_7$ film with the c-axis orientation on LAO substrate was obtained as a byproduct. Although the grown films exhibit semiconducting behavior without superconducting transitions, carrier tuning via O_3 annealing may provide an effective route to induce superconductivity in $La_4Ni_3O_{10}$ films, representing a promising direction for future study.

Supplementary Material

The detailed parameters of PLD growth, the TEM image with EDX mapping near the boundary between the deposited film and the substrate in the $La_4Ni_3O_{10}$ film, and the gradually increasing

resistance behavior of the $La_4Ni_3O_{10}$ film after O_3 annealing are shown in the SM.

Acknowledgement

This work was partly supported by JSPS KAKENHI Grant Number 23H01835, 23K13549, 23KK0088, 25K01508, and JST K Program Grant Number JPMJKP25Z2. The TEM observation was carried out with the support of "Advanced Research Infrastructure for Materials and Nanotechnology in Japan (ARIM)" of the Ministry of Education, Culture, Sports, Science and Technology (MEXT) with Proposal Number JPMXP1225NM5218. The XRD analysis was supported by Dr. T. Hiroto in Materials Fabrication and Analysis Platform of NIMS. This work was supported by NIMS Joint Research Hub Program and the World Premier International Research Center Initiative (WPI), MEXT, Japan.

Data Availability

The data that supports the findings of this study are available from the corresponding author upon reasonable request.

References

[1] S.A. Chambers, "Epitaxial Growth and Properties of Doped Transition Metal and Complex Oxide Films," Advanced Materials **22**(2), 219–248 (2010).

[2] J.V. Mantese, A.L. Micheli, A.H. Hamdi, and R.W. Vest, "Metalorganic Deposition (MOD): A Nonvacuum, Spin-on, Liquid-Based, Thin Film Method," MRS Bull. **14**(10), 48–53 (1989).

[3] M. Cazzanelli, D. Cole, J. Versluijs, J.F. Donegan, and J.G. Lunney, "Pulsed laser deposition of GaN thin films," Materials Science and Engineering: B **59**(1–3), 98–103 (1999).

[4] J. Kawamura, N. Kuwata, K. Toribami, N. Sata, O. Kamishima, and T. Hattori, "Preparation of amorphous lithium ion conductor thin films by pulsed laser deposition," Solid State Ionics **175**(1–4), 273–276 (2004).

[5] D. Mouloua, J. LeBlanc-Lavoie, L. Pichon, N.S. Rajput, M. El Marssi, M. Jouiad, and M.A. El Khakani, "Tuning the Optoelectronic Properties of Pulsed Laser Deposited '3D'-MoS_2 Films via the Degree of Vertical Alignment of Their Constituting Layers," Advanced Optical Materials **12**(15), 2302966 (2024).

[6] D. Dijkkamp, T. Venkatesan, X.D. Wu, S.A. Shaheen, N. Jisrawi, Y.H. Min-Lee, W.L. McLean, and M. Croft, "Preparation of Y-Ba-Cu oxide superconductor thin films using pulsed laser evaporation from high T_c bulk material," Applied Physics Letters **51**(8), 619–621 (1987).

[7] H.M. Christen, and G. Eres, "Recent advances in pulsed-laser deposition of complex oxides," J. Phys.: Condens. Matter **20**(26), 264005 (2008).

[8] N.A. Shepelin, Z.P. Tehrani, N. Ohannessian, C.W. Schneider, D. Pergolesi, and T. Lippert, "A practical guide to pulsed laser deposition," Chem. Soc. Rev. **52**(7), 2294–2321 (2023).

[9] J.H. Haeni, P. Irvin, W. Chang, R. Uecker, P. Reiche, Y.L. Li, S. Choudhury, W. Tian, M.E. Hawley, B. Craigo, A.K. Tagantsev, X.Q. Pan, S.K. Streiffer, L.Q. Chen, S.W. Kirchoefer, J. Levy, and D.G. Schlom, "Room-temperature ferroelectricity in strained SrTiO3," Nature **430**(7001), 758–761 (2004).

[10] J.-M. Bassat, M. Burriel, O. Wahyudi, R. Castaing, M. Ceretti, P. Veber, I. Weill, A. Villesuzanne, J.-C. Grenier, W. Paulus, and J.A. Kilner, "Anisotropic Oxygen Diffusion Properties in $Pr_2 NiO_{4+\delta}$ and $Nd_2 NiO_{4+\delta}$ Single Crystals," J. Phys. Chem. C **117**(50), 26466–26472 (2013).

[11] H. Sun, M. Huo, X. Hu, J. Li, Z. Liu, Y. Han, L. Tang, Z. Mao, P. Yang, B. Wang, J. Cheng, D.-X. Yao, G.-M. Zhang, and M. Wang, "Signatures of superconductivity near 80 K in a nickelate under high pressure," Nature **621**(7979), 493–498 (2023).

[12] P. Puphal, P. Reiss, N. Enderlein, Y.-M. Wu, G. Khaliullin, V. Sundaramurthy, T. Priessnitz, M. Knauft, A. Suthar, L. Richter, M. Isobe, P.A. Van Aken, H. Takagi, B. Keimer, Y.E. Suyolcu, B. Wehinger, P. Hansmann, and M. Hepting, "Unconventional Crystal Structure of the High-Pressure Superconductor La 3 Ni 2 O 7," Phys. Rev. Lett. **133**(14), 146002 (2024).

[13] H. Sakakibara, N. Kitamine, M. Ochi, and K. Kuroki, "Possible High T c Superconductivity in La 3 Ni 2 O 7 under High Pressure through Manifestation of a Nearly Half-Filled Bilayer Hubbard Model," Phys. Rev. Lett. **132**(10), 106002 (2024).

[14] M. Kakoi, T. Oi, Y. Ohshita, M. Yashima, K. Kuroki, T. Kato, H. Takahashi, S. Ishiwata, Y. Adachi, N. Hatada, T. Uda, and H. Mukuda, "Multiband Metallic Ground State in Multilayered Nickelates $La_3 Ni_2 O_7$ and $La_4 Ni_3 O_{10}$ Probed by^{139} La-NMR at Ambient Pressure," J. Phys. Soc. Jpn. **93**(5), 053702 (2024).

[15] Z. Pan, C. Lu, F. Yang, and C. Wu, "Effect of Rare-Earth Element Substitution in Superconducting $R_3 Ni_2 O_7$ under Pressure," Chinese Phys. Lett. **41**(8), 087401 (2024).

[16] Z. Huo, P. Zhang, H. Shi, X. Yan, D. Duan, and T. Cui, "First-principles study of the Pr-doped bilayer nickelate L a 3 N i 2 O 7," Phys. Rev. B **111**(19), 195118 (2025).

[17] F. Li, Z. Xing, D. Peng, J. Dou, N. Guo, L. Ma, Y. Zhang, L. Wang, J. Luo, J. Yang, J. Zhang, T. Chang, Y.-S. Chen, W. Cai, J. Cheng, Y. Wang, Y. Liu, T. Luo, N. Hirao, T. Matsuoka, H. Kadobayashi, Z. Zeng, Q. Zheng, R. Zhou, Q. Zeng, X. Tao, and J. Zhang, "Bulk superconductivity up to 96 K in pressurized nickelate single crystals," Nature **649**(8098), 871–878 (2026).

[18] Y. Ueki, H. Sakurai, H. Nagata, K. Yamane, R. Matsumoto, K. Terashima, K. Hirose, H. Ohta, M. Kato, and Y. Takano, "Phase Diagram of Pressure-Induced High Temperature Superconductor $La_3 Ni_2 O_{7+\delta}$," J. Phys. Soc. Jpn. **94**(1), 013703 (2025).

[19] K. Yamane, Y. Matsushita, S. Adachi, T. Hiroto, R. Matsumoto, K. Terashima, H. Sakurai, and Y. Takano, "High-pressure synthesis of bilayer nickelate $Sr_3 Ni_2 O_5 Cl_2$ with a tetragonal crystal structure," Acta Crystallogr C Struct Chem **81**(5), 259–263 (2025).

[20] Y. Zhang, D. Su, Y. Huang, Z. Shan, H. Sun, M. Huo, K. Ye, J. Zhang, Z. Yang, Y. Xu, Y. Su, R. Li, M. Smidman, M. Wang, L. Jiao, and H. Yuan, "High-temperature superconductivity with zero-resistance and strange metal behavior in $La_3Ni_2O_{7-\delta}$," Nat. Phys. **20**(8), 1269–1273 (2024).

[21] Y. Shen, M. Qin, and G.-M. Zhang, "Effective Bi-Layer Model Hamiltonian and Density-Matrix Renormalization Group Study for the High-T_c Superconductivity in $La_3 Ni_2 O_7$ under High Pressure," Chinese Phys. Lett. **40**(12), 127401 (2023).

[22] G. Zhou, W. Lv, H. Wang, Z. Nie, Y. Chen, Y. Li, H. Huang, W.-Q. Chen, Y.-J. Sun, Q.-K. Xue, and Z. Chen, "Ambient-pressure superconductivity onset above 40 K in $(La,Pr)_3Ni_2O_7$ films," Nature **640**(8059), 641–646 (2025).

[23] E.K. Ko, Y. Yu, Y. Liu, L. Bhatt, J. Li, V. Thampy, C.-T. Kuo, B.Y. Wang, Y. Lee, K. Lee, J.-S. Lee, B.H. Goodge, D.A. Muller, and H.Y. Hwang, "Signatures of ambient pressure superconductivity in thin film $La_3Ni_2O_7$," Nature **638**(8052), 935–940 (2025).

[24] Y. Liu, E.K. Ko, Y. Tarn, L. Bhatt, J. Li, V. Thampy, B.H. Goodge, D.A. Muller, S. Raghu, Y. Yu, and H.Y. Hwang, "Superconductivity and normal-state transport in compressively strained La2PrNi2O7 thin films," Nat. Mater. **24**(8), 1221–1227 (2025).

[25] H. Sakakibara, M. Ochi, H. Nagata, Y. Ueki, H. Sakurai, R. Matsumoto, K. Terashima, K. Hirose, H. Ohta, M. Kato, Y. Takano, and K. Kuroki, "Theoretical analysis on the possibility of superconductivity in the trilayer Ruddlesden-Popper nickelate $La_4Ni_3O_{10}$ under pressure and its experimental examination: Comparison with $La_3Ni_2O_7$," Phys. Rev. B **109**(14), 144511 (2024).

[26] M. Zhang, C. Pei, D. Peng, X. Du, W. Hu, Y. Cao, Q. Wang, J. Wu, Y. Li, H. Liu, C. Wen, J. Song, Y. Zhao, C. Li, W. Cao, S. Zhu, Q. Zhang, N. Yu, P. Cheng, L. Zhang, Z. Li, J. Zhao, Y. Chen, C. Jin, H. Guo, C. Wu, F. Yang, Q. Zeng, S. Yan, L. Yang, and Y. Qi, "Superconductivity in Trilayer Nickelate La 4 Ni 3 O 10 under Pressure," Phys. Rev. X **15**(2), 021005 (2025).

[27] Y. Zhu, D. Peng, E. Zhang, B. Pan, X. Chen, L. Chen, H. Ren, F. Liu, Y. Hao, N. Li, Z. Xing, F. Lan, J. Han, J. Wang, D. Jia, H. Wo, Y. Gu, Y. Gu, L. Ji, W. Wang, H. Gou, Y. Shen, T. Ying, X. Chen, W. Yang, H. Cao, C. Zheng, Q. Zeng, J. Guo, and J. Zhao, "Superconductivity in pressurized trilayer La4Ni3O10−δ single crystals," Nature **631**(8021), 531–536 (2024).

[28] F. Li, Y. Hao, N. Guo, D. Jia, J. Dou, D. Peng, G. Zhang, L. Xiao, J. Zhang, W. Zhou, Y. Huang, X. Wang, Z. Guo, M. Mezouar, J. Elias F. S. Rodrigues, J. Luo, J. Yang, Q. Zeng, R. Zhou, H. Gou, Q. Zheng, G. Liu, and J. Zhang, "Single-Crystal Structure Determination of Superconducting La_4 Ni_3 $O_{10-\delta}$ under High Pressure," Advanced Materials **37**(44), e07365 (2025).

[29] M. Osada, C. Terakura, A. Kikkawa, M. Nakajima, H.-Y. Chen, Y. Nomura, Y. Tokura, and A. Tsukazaki, "Strain-tuning for superconductivity in La3Ni2O7 thin films," Commun Phys **8**(1), 251 (2025).

[30] K.-T. Wu, Y.-A. Soh, and S.J. Skinner, "Epitaxial growth of mixed conducting layered Ruddlesden–Popper Lan+1NinO3n+1 (n=1, 2 and 3) phases by pulsed laser deposition," Materials Research Bulletin **48**(10), 3783–3789 (2013).

[31] Z. Li, W. Guo, T.T. Zhang, J.H. Song, T.Y. Gao, Z.B. Gu, and Y.F. Nie, "Epitaxial growth and electronic structure of Ruddlesden–Popper nickelates (La n +1Ni n O3 n +1, n = 1–5)," APL Materials **8**(9), 091112 (2020).

[32] M. Zinkevich, N. Solak, H. Nitsche, M. Ahrens, and F. Aldinger, "Stability and thermodynamic functions of lanthanum nickelates," Journal of Alloys and Compounds **438**(1–2), 92–99 (2007).

[33] M.C. Foote, B.B. Jones, B.D. Hunt, J.B. Barner, R.P. Vasquez, and L.J. Bajuk, "Composition variations in pulsed-laser-deposited Y-Ba-Cu-O thin films as a function of deposition parameters," Physica C: Superconductivity **201**(1–2), 176–182 (1992).